

Thermodynamic Constraints on Reductive Reactions Influencing the Biogeochemistry of Arsenic in Soils and Sediments

BENJAMIN D. KOCAR AND
SCOTT FENDORF*

*Environmental Earth System Science, Stanford University,
Stanford, California 94305*

*Received December 13, 2008. Revised manuscript received
March 13, 2009. Accepted April 15, 2009.*

Arsenic is a widespread environmental toxin having devastating impacts on human health. A transition to anaerobic conditions is a key driver for promoting As desorption through either the reduction of As(V) or the reductive dissolution of Fe(III) (hydr)oxides. However, a disparity in the reported release sequence for As and Fe to the aqueous solution hinders our ability to determine the controlling factors liberating As to the aqueous environment. Accordingly, we performed a thermodynamic analysis of Fe, using a range of Fe-(hydr)oxides, and As reduction coupled with hydrogen, acetate, and lactate oxidation for a range of relevant field conditions. The favorability of sulfate reduction is also evaluated. Our results illustrate that As reduction is favorable over a wide-range of field conditions, and Fe reduction is differentially favorable depending on the buildup of metabolites (mainly Fe²⁺) and the Fe (hydr)oxide being reduced; reduction of As(V) is thermodynamically favorable under most environmental conditions and almost always more favorable than goethite and hematite reduction. Sulfate reduction is favorable over a range of conditions, and may occur concomitantly with Fe reduction depending on the Fe (hydr)oxides present. Thus, on a thermodynamic basis, the general sequence of microbial reduction should be As(V) followed by Fe(III) or sulfate.

Introduction

Arsenic is a toxic metalloid poisoning millions of people worldwide (1). Although notable and problematic contamination occurs from anthropogenic activities (e.g., mining, As-pesticides, and manufacturing), consumption of naturally occurring As in groundwater is the dominant pathway of human exposure globally (2). Reductive transformation/dissolution of As(V) and Fe(III) (hydr)oxides are considered the primary mechanisms of solubilization in most surface and subsurface environments, and they are a principal mechanism of arsenic release to groundwaters of South and Southeast Asia (3–6).

Arsenic reduction can occur through two biotic mechanisms: respiration and detoxification. In respiration, catabolic As reduction is coupled to the oxidation of organic carbon or hydrogen. In detoxification, As(V) imported into the cell is reduced and then expelled from the cell via an As(III)-specific efflux pump (7). Both mechanisms may be

operational under anaerobic soil conditions, but the detoxification mechanism commences at relatively high As concentrations (~100 μM) (8). Thus, at lower concentrations, As reduction likely occurs through respiratory pathways and is therefore subject to thermodynamic constraints (e.g., As(V) reduction must be favorable to yield energy gain by the bacterium).

Iron reduction is often an exergonic process when linked to carbon or hydrogen oxidation, but the cellular processes governing this reaction are less understood. The terminal reductase of the genus *Geobacter* and *Shewanella* species, for example, are thought to consist of outer-membrane cytochromes which directly transfer electrons to Fe(III)_(s) (9, 10). However, extra-cellular electron carriers, such as Fe(III)-bearing humic acids and redox-active (quinone-like) molecules have also been suggested as capable of transferring electrons appreciable distances to Fe(III)_(s) (11, 12), and more recently, flavins were shown as possible endogenous electron shuttles in *Shewanella* species (13, 14). Ultimately, Fe reduction may be governed by the thermodynamic properties of the Fe (hydr)oxide being reduced for the specific reaction mechanism. Generally, poorly crystalline Fe (hydr)oxides such as ferrihydrite yield higher energy gains by bacteria than more crystalline phases, such as goethite or hematite (15).

Reduction of As(V) and Fe(III) are generally postulated to transpire at similar redox potentials, but the reduction sequence, viewed through production of dissolved As(III) and Fe(II), varies (see, for example, ref 4). While kinetic factors may often determine observed Fe(III) and As(V) reduction, thermodynamic viability has an overriding control on whether a reaction can proceed and on energy yield for respiration. At present, there is a paucity of data regarding the thermodynamic favorability of processes representative of field conditions. We therefore performed a thermodynamic evaluation of Fe(III) (hydr)oxide and As(V) reduction; sulfate reduction may also impact the fate of both As and Fe, and we thus include this redox active constituent in our analysis. To place our thermodynamic calculations in the direct context of field conditions, we evaluate reaction favorability(s) using solid and aqueous phase measurements from a field site in Cambodia, where As release from shallow (<4m) sediments is known to occur (3, 6, 16).

Hydrogen, acetate and lactate were evaluated as electron donors based on the partial equilibrium approach for examining electron donor and acceptor utilization within sediments (17, 18). The partial equilibrium approach assumes that the rate limiting step driving biogeochemical reactions is the fermentation of organic matter, and that the kinetics of fermentation, and resulting production of small molecular weight carbon species (e.g., acetate, lactate, etc.) and hydrogen are slow compared to the kinetics of TEA reduction. The electron accepting processes are therefore close to equilibrium, while organic matter fermentation is not. Partial equilibrium has been successfully invoked to describe a variety of geochemical processes occurring within sediments and aquifers (17–19).

Our analysis illustrates that As, Fe, and S reduction are all thermodynamically viable over a wide-range of field conditions and that electron donor, metabolite concentrations, and pH exert a strong control on reaction favorability. With the exception of very low As(V) and Fe(II) activities, As reduction is more favorable than goethite and hematite reduction, and is more favorable than ferrihydrite reduction above (Fe²⁺) of ~1.0 × 10⁻⁵. The favorability of sulfate and Fe(III) reduction, however, vary depending on geochemical

* Corresponding author phone: 650-723-5238; e-mail: fendorf@stanford.edu.

TABLE 1. Gibbs Free Energy of Formation for Reaction Constituents

constituent	ΔG_f° (kJ/mol)	reference
Fe(OH) ₃ (am)	-708.5	39
FeOOH	-489.8	40
Fe ₂ O ₃	-746.2	41
Fe ²⁺	-91.50	42
C ₃ H ₅ O ₃ ⁻	-512.67	42
C ₂ H ₃ O ₂ ⁻	-369.33	42
HAsO ₄ ²⁻	-714.59	42
H ₂ AsO ₄ ²⁻	-753.17	42
H ₃ AsO ₃	-587.13	43
HCO ₃ ⁻	-586.94	42
H ₂ O	-237.17	42
SO ₄ ²⁻	-744.46	42
HS ⁻	11.97	42
H ₂ (aq)	17.72	42
Fe(OH) ₂ ⁺	-438	23

conditions, as noted previously (19), and the type of Fe mineral. The reduction of Fe(III) and sulfate ultimately impacts the fate of As through potential secondary precipitation or adsorption reactions.

Modeling and Field Validation Approach.

Thermodynamic Calculations. The standard state Gibbs free energy of reactions was determined from compiled values for relevant reaction constituents (Tables 1 and 2). Given the variation in solubility (and thus, ΔG_f°) of natural Fe (hydr)oxides, $\Delta G^\circ_{\text{rxn}}$ values for the reduction of Fe (hydr)oxides coupled to hydrogen oxidation across a range of Fe (hydr)oxide solubilities are tabulated and compared to $\Delta G^\circ_{\text{rxn}}$ values calculated with ΔG_f° of synthetic Fe (hydr)oxides (see Supporting Information (SI)). Concentrations of field-relevant aqueous constituents were adjusted to activities using coefficients calculated with the Davies equation, and the nonstandard state Gibbs free energy of reaction was then obtained using the Lewis equation (eq 1) at 298 K and 1 atm pressure:

$$\Delta G = \Delta G^\circ + RT(\ln 10)\log(Q) = \Delta G^\circ + 5.7081 \times \log(Q) \quad (1)$$

The reaction quotient, Q , is defined for a reaction as

$$a(A) + b(B) = c(C) + d(D) \quad (2)$$

$$Q = \frac{(C)^c(D)^d}{(A)^a(B)^b} \quad (3)$$

Non-standard state conditions for As(V), S(VI), and Fe(III)_(s) reduction coupled to hydrogen, acetate, and lactate oxidation were examined. Gibbs free energies of reaction were calculated for field-relevant concentrations; for (H₂(aq)), 1.0 × 10⁻⁹ was chosen, which is representative of H₂(aq) concentrations found under iron reducing conditions (20); acetate was evaluated at 9.0 × 10⁻⁶ (21), and lactate, typically found at much lower concentrations than acetate, was evaluated at 9.0 × 10⁻⁷ (22). The sensitivity of Gibbs free energy for As(V), Fe(III), and S(VI) reduction analyses to varying electron donor is presented in the SI. These analysis, which bracket a wide range of values (two or more orders of magnitude), illustrate that large variations in electron donor concentration do not change the hierarchy of free energy gain between reductive reactions, and large changes in (H₂(aq)), (acetate) and (lactate) are required to substantially change the magnitude of ΔG_{rxn} .

Site Description and Sample Collection. Solid and aqueous phase measurements from a field site in Kandal Province, Cambodia were used to validate the thermodynamic analysis. Methods of sample collection, chemical and spectroscopic analysis and the hydrology of the system, including sampling

site locations (denoted sites A and T) were previously described (3, 6, 16). A brief description and a methodological synopsis is provided in the SI.

Results and Discussion

Standard versus Reaction State Thermodynamic Favorability. Biogeochemical reactions yielding the greatest Gibbs free energy will dominate until reactants are depleted, at which time the dominant process will cycle to the next most favorable energy yielding reaction (23). Under standard state conditions, the Gibbs free energy of reaction for ferrihydrite and singly protonated arsenate (HAsO₄²⁻) are the most favorable on a per mol electron donor basis for hydrogen, acetate, and lactate oxidation, followed by goethite, hematite, diprotonated arsenate (H₂AsO₄²⁻), and finally, sulfate reduction (Table 2). However, the driving force for reaction will depend not only on the intrinsic reaction favorability (standard state conditions) but also on the concentration gradients established by the reactants and products, such as Fe²⁺ accumulation during Fe (hydr)oxide reduction (Figure 1). The Gibbs free energy of reaction for As, Fe, and S reduction, for example, will change by ~10 kJ/mol with each 100-fold change in acetate concentration (SI Figure 4SI); changing the product concentrations of each reaction, including As(III) (As reduction), Fe²⁺ (Fe reduction), HS⁻ (sulfate reduction), and acetate (lactate oxidation) will also decrease the favorability of each reaction accordingly. When pH is varied (Figure 2), favorability changes dramatically, with the Gibbs free energy yield decreasing according to the stoichiometry of proton consumption or production (Table 2). The Gibbs free energy of reaction is particularly sensitive to reaction constituents with high stoichiometric coefficients—as noted in eq 3 (e.g., proton consumption with goethite or hematite reduction coupled to acetate oxidation, reactions 11 and 12, Table 2).

On the basis of the Gibbs free energy calculated for reaction conditions, As(V) (either HAsO₄²⁻ or H₂AsO₄⁻ at circumneutral pH, pK_{a2} = 6.8) reduction is the most favorable reaction across a range of As, H₂, lactate, acetate, and pH values representative of possible field conditions (Figures 1 and 2). As previously noted (24), ferrihydrite reduction is the only process listed here which yields similar Gibbs free energy to As(V) reduction; ferrihydrite reduction, however, is more favorable than As(V) only at high As(III):As(V) ratios (Figure 2), and the relative favorability diminishes markedly at Fe²⁺ activities greater than 8 × 10⁻⁶ (Figure 1). On a thermodynamic basis, As reduction is therefore generally expected to occur regardless of the presence of reducible Fe(III)_(s) or sulfate, and will likely only be inhibited in the presence of high O₂ or NO₃⁻.

Relative Favorability of Iron(III) and Sulfate Reduction.

The energy yield of ferrihydrite coupled to H₂, acetate or lactate oxidation is substantially higher than hematite, goethite, and sulfate reduction at low Fe²⁺ concentrations. Conversely, the favorability of sulfate reduction exceeds that of goethite and hematite reduction at ~5.0 × 10⁻⁵ Fe²⁺, and approaches that of ferrihydrite reduction at high pH or very high Fe²⁺ concentration (Figures 1 and 2), albeit that the Fe²⁺ concentrations required for this to occur are typically not observed under field conditions (>1 × 10⁻³ at pH 7, Figure 1). It is therefore expected that ferrihydrite reduction will be more favorable than that of sulfate, since Fe(II)-bearing minerals (e.g., siderite) typically regulate dissolved Fe²⁺ (see below).

The favorability of sulfate reduction exceeds the favorability of goethite and hematite reduction at elevated (yet commonly observed) Fe²⁺ concentrations (~5.0 × 10⁻⁵) when coupled with hydrogen, acetate, or lactate oxidation, and may therefore proceed as the dominant biogeochemical reaction in aged sediments dominated by crystalline Fe

TABLE 2. Standard State Gibbs Free Energy for Pertinent Reactions

	reactions considered	$\Delta G^\circ_{\text{rxn}}$ (kJ/mol)
Hydrogen Oxidation Reactions		
1	$2\text{Fe}(\text{OH})_3 + \text{H}_{2(\text{aq})} + 4\text{H}^+ \rightarrow 2\text{Fe}^{2+} + 6\text{H}_2\text{O}$	-206.7
2	$\text{HAsO}_4^{2-} + \text{H}_{2(\text{aq})} + 2\text{H}^+ \rightarrow \text{H}_3\text{AsO}_3 + \text{H}_2\text{O}$	-180.0
3	$2\text{FeOOH} + \text{H}_{2(\text{aq})} + 4\text{H}^+ \rightarrow 2\text{Fe}^{2+} + 4\text{H}_2\text{O}$	-169.8
4	$2\text{Fe}_2\text{O}_3 + \text{H}_{2(\text{aq})} + 4\text{H}^+ \rightarrow 2\text{Fe}^{2+} + 3\text{H}_2\text{O}$	-166.0
5	$\text{H}_2\text{AsO}_4 + \text{H}_{2(\text{aq})} + \text{H}^+ \rightarrow \text{H}_3\text{AsO}_3 + \text{H}_2\text{O}$	-141.5
6	$0.25\text{SO}_4^{2-} + \text{H}_{2(\text{aq})} + 0.25\text{H}^+ \rightarrow 0.25\text{HS}^- + \text{H}_2\text{O}$	-65.8
7	$2\text{Fe}(\text{OH})_2^+ + \text{H}_{2(\text{aq})} \rightarrow 2\text{Fe}^{2+} + 2\text{H}_2\text{O}$	-255.7
8	$2\text{Fe}(\text{III})(\text{citrate}) + \text{H}_{2(\text{aq})} \rightarrow 2\text{Fe}(\text{II})(\text{citrate})^- + 2\text{H}^+$	-53.5 ^a
Acetate Oxidation Reactions		
9	$8\text{Fe}(\text{OH})_3 + \text{CH}_3\text{COO}^- + 15\text{H}^+ \rightarrow 8\text{Fe}^{2+} + 2\text{HCO}_3^- + 20\text{H}_2\text{O}$	-612.0
10	$4\text{HAsO}_4^{2-} + \text{CH}_3\text{COO}^- + 7\text{H}^+ \rightarrow 4\text{H}_3\text{AsO}_3 + 2\text{HCO}_3^-$	-505.1
11	$8\text{FeOOH} + \text{CH}_3\text{COO}^- + 15\text{H}^+ \rightarrow 8\text{Fe}^{2+} + 2\text{HCO}_3^- + 12\text{H}_2\text{O}$	-464.2
12	$4\text{Fe}_2\text{O}_3 + \text{CH}_3\text{COO}^- + 15\text{H}^+ \rightarrow 8\text{Fe}^{2+} + 2\text{HCO}_3^- + 8\text{H}_2\text{O}$	-449.1
13	$4\text{H}_2\text{AsO}_4^- + \text{CH}_3\text{COO}^- + 3\text{H}^+ \rightarrow 4\text{H}_3\text{AsO}_3 + 2\text{HCO}_3^-$	-350.8
14	$\text{SO}_4^{2-} + \text{CH}_3\text{COO}^- \rightarrow \text{HS}^- + 2\text{HCO}_3^-$	-48.1
15	$8\text{Fe}(\text{OH})_2^+ + \text{CH}_3\text{COO}^- + 7\text{H}^+ \rightarrow 8\text{Fe}^{2+} + 2\text{HCO}_3^- + 12\text{H}_2\text{O}$	-878.6
16	$8\text{Fe}(\text{III})(\text{citrate}) + \text{CH}_3\text{COO}^- + 4\text{H}_2\text{O} \rightarrow 8\text{Fe}(\text{II})(\text{citrate})^- + 2\text{HCO}_3^- + 9\text{H}^+$	-344.5 ^a
Lactate Oxidation Reactions		
17	$4\text{Fe}(\text{OH})_3 + \text{C}_3\text{H}_5\text{O}_3^- + 7\text{H}^+ \rightarrow 4\text{Fe}^{2+} + \text{CH}_3\text{COO}^- + \text{HCO}_3^- + 10\text{H}_2\text{O}$	-347.3
18	$2\text{HAsO}_4^{2-} + \text{C}_3\text{H}_5\text{O}_3^- + 3\text{H}^+ \rightarrow 2\text{H}_3\text{AsO}_3 + \text{CH}_3\text{COO}^- + \text{HCO}_3^-$	-293.9
19	$4\text{FeOOH} + \text{C}_3\text{H}_5\text{O}_3^- + 7\text{H}^+ \rightarrow 4\text{Fe}^{2+} + \text{CH}_3\text{COO}^- + \text{HCO}_3^- + 6\text{H}_2\text{O}$	-273.4
20	$4\text{Fe}_2\text{O}_3 + \text{C}_3\text{H}_5\text{O}_3^- + 7\text{H}^+ \rightarrow 4\text{Fe}^{2+} + \text{CH}_3\text{COO}^- + \text{HCO}_3^- + 4\text{H}_2\text{O}$	-265.9
21	$2\text{H}_2\text{AsO}_4^- + \text{C}_3\text{H}_5\text{O}_3^- + \text{H}^+ \rightarrow 2\text{H}_3\text{AsO}_3 + \text{CH}_3\text{COO}^- + \text{HCO}_3^-$	-216.7
22	$0.5\text{SO}_4^{2-} + \text{C}_3\text{H}_5\text{O}_3^- \rightarrow 0.5\text{HS}^- + \text{CH}_3\text{COO}^- + \text{HCO}_3^- + 0.5\text{H}^+$	-65.4

^a Calculated by combining iron and hydrogen half reactions with Fe-citrate complexation reactions presented by Liu et al. (44)

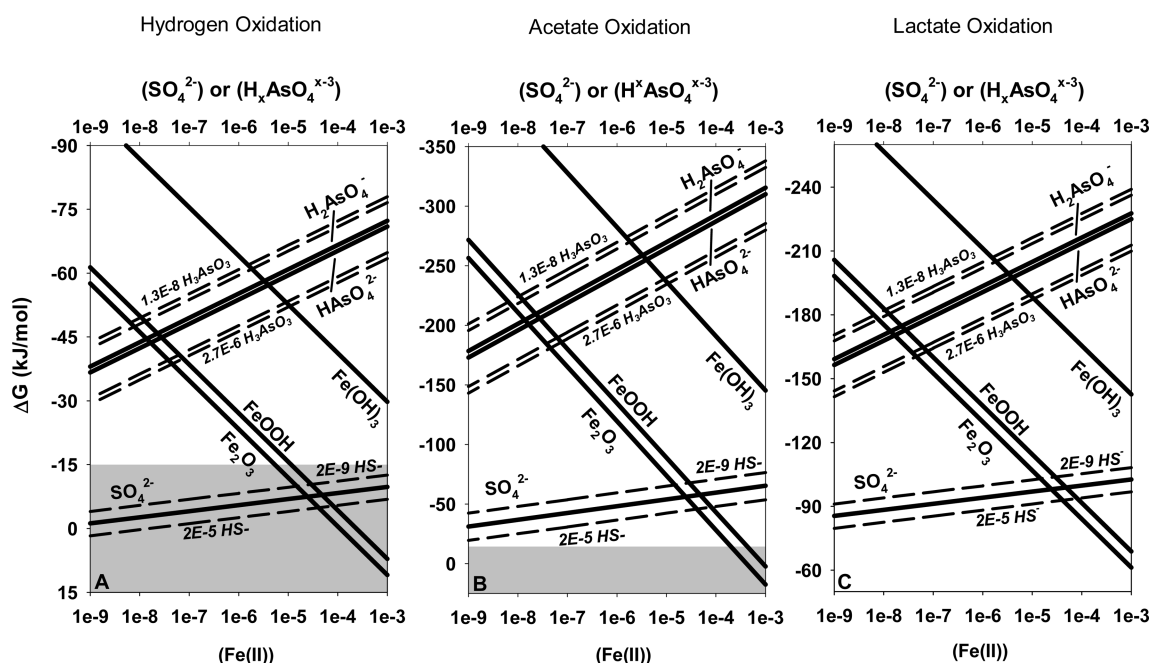


FIGURE 1. (A) ΔG_{rxn} calculated for As(V), S(VI), and Fe(III)_(s) reduction coupled with (A) H₂ (B) acetate and (C) lactate oxidation at pH 7.0 as a function of H₂AsO₄^{x-3}/HAsO₄^{x-3}, SO₄²⁻ and Fe²⁺. For hydrogen oxidation reactions, H₂ = 1.0 × 10⁻⁹; for acetate oxidation reactions (HCO₃⁻) = 7.1 × 10⁻³ and (CH₃COO⁻) = 9.0 × 10⁻⁶; and for incomplete lactate oxidation reactions, (HCO₃⁻) = 7.1 × 10⁻³, (C₃H₅O₃⁻) = 9.0 × 10⁻⁷ and (CH₃COO⁻) = 9.0 × 10⁻⁶. Dashed lines bracketing As(V) reduction favorability are ΔG_{rxn} calculated with H₃AsO₃ activities of 1.3 × 10⁻⁸ and 2.7 × 10⁻⁶ (solid line is ΔG_{rxn} favorability at 1.3 × 10⁻⁷ H₃AsO₃). Dashed lines bracketing SO₄²⁻ reduction favorability are ΔG_{rxn} values calculated with HS⁻ activities of 2.0 × 10⁻⁹ and 2.0 × 10⁻⁵ (solid line is ΔG_{rxn} favorability at 2.0 × 10⁻⁷). Shaded boxes within all plots represent ΔG_{rxn} values below the nominal minimum threshold required for metabolic maintenance (35, 37).

(hydr)oxides. At H₂ activities of 1 × 10⁻⁹, hematite and goethite reduction is marginally (0 to -15 kJ/mol) favorable above Fe²⁺ activities of ~1 × 10⁻⁵, but is appreciably more favorable at elevated H₂ (10⁻⁷ atm, see SI Figure 4SI). Sulfate reduction is also marginally favorable at 10⁻⁹ atm H₂, (-15–0 kJ/mol) (Figure 1 and SI Figure 4SI). However, As(V) reduction

is favorable over a wide range of H_{2(aq)} and As(V) activities, even with low As(V) and H_{2(aq)} (<1.0 × 10⁻⁸ As(V) and 1 × 10⁻¹¹ H₂, SI Figure 4SI).

The reduction of hematite by acetate (Reaction 12, Table 2) yields -449.1 kJ/mol at standard state, but when adjusted to high Fe²⁺ activities (approximately 3.0 × 10⁻⁴), the reaction

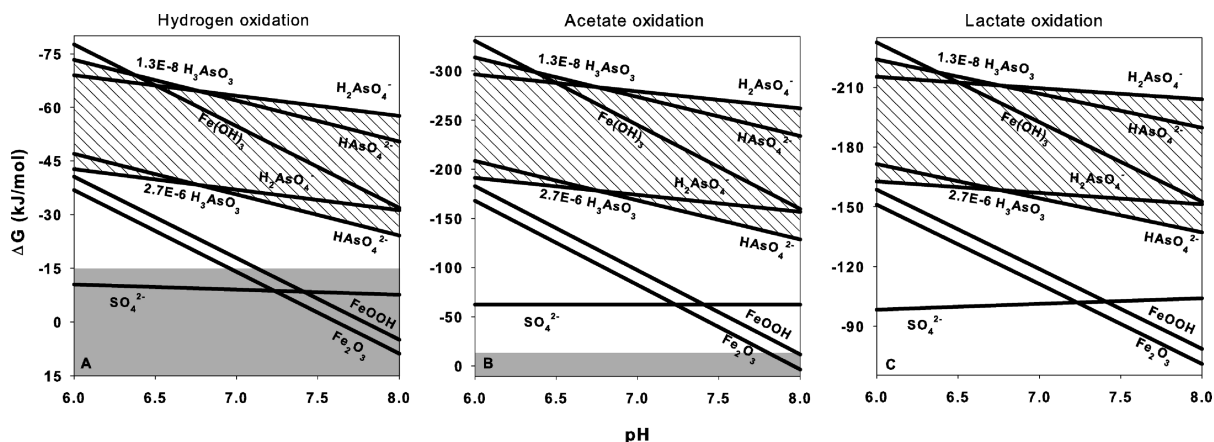


FIGURE 2. ΔG_{rxn} calculated as a function of pH for As(V), S(VI), and Fe(III)_(s) reduction coupled with (A) hydrogen, (B) acetate, and (C) lactate oxidation. For hydrogen oxidation reactions $H_2 = 1.0 \times 10^{-9}$; for acetate oxidation reactions $(HCO_3^-) = 7.1 \times 10^{-3}$ and $(CH_3COO^-) = 9.0 \times 10^{-6}$; for incomplete lactate oxidation reactions $(HCO_3^-) = 7.1 \times 10^{-3}$, $(CH_3COO^-) = 9.0 \times 10^{-6}$ and $(C_3H_5O_3^-) = 9.0 \times 10^{-7}$. In each case, $(Fe^{2+}) = 6.5 \times 10^{-6}$, $(SO_4^{2-}) = 3.24 \times 10^{-4}$, $(HS^-) = 1.78 \times 10^{-7}$, and $(As(V)) = 6.0 \times 10^{-6}$. To demonstrate the effect of varying As(III):As(V), As(V) reduction favorability is calculated with $(H_3AsO_3) = 1.3 \times 10^{-8}$ and 2.7×10^{-6} , and the range of ΔG_{rxn} between these calculations falls within the cross-hatched area. Shaded boxes within all plots represent ΔG_{rxn} values below the nominal minimum threshold required for metabolic maintenance (35, 37).

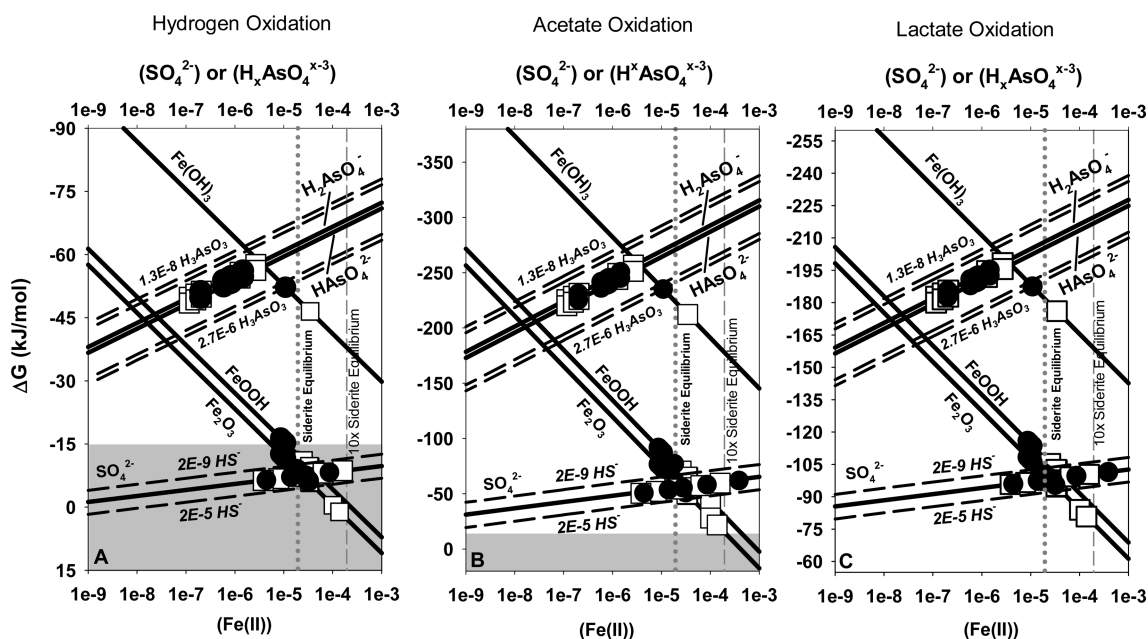


FIGURE 3. Solid lines for (A) hydrogen, (B) acetate, and (C) lactate oxidation reactions are identical to those calculated in Figure 1. Calculated ΔG_{rxn} values (point data) for Fe, As, and S reduction are plotted based on field measurements of aqueous and solid phases reaction constituents. Open squares and closed circles represent ΔG_{rxn} values calculated from sediment chemistry collected from different locations (Sites A and T, respectively) where As release from sediments is known to occur (see SI). Vertical dotted lines represent $Fe^{2+}(aq)$ concentrations in equilibrium or 10 times oversaturated with respect to siderite (dashed line in each graph). Shaded boxes within all plots represent ΔG_{rxn} values below the nominal minimum threshold required for metabolic maintenance (35, 37).

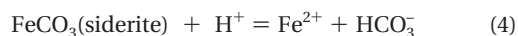
becomes unfavorable (Figure 3). When coupled to hydrogen oxidation, the thermodynamic control of Fe^{2+} on hematite reduction is more striking; goethite reduction becomes unfavorable above Fe^{2+} activities of 8×10^{-6} , which is observed under field conditions (Figure 3). Bacteria therefore utilizing acetate (and hydrogen) as a substrate at elevated Fe^{2+} levels will be required to use a different electron acceptor (e.g., ferrihydrite) or a multistep (dissolution followed by reduction) reaction pathway. To reduce hematite, an alternate electron donor or reaction path would be needed. Indeed, lactate oxidation coupled to hematite reduction under the same field conditions is favorable, yielding approximately -70 kJ/mol at (Fe^{2+}) of 3.0×10^{-4} ; other fermentation products or aromatic and aliphatic hydrocarbons may also provide favorable energy yields when linked to hematite

reduction (25). A suite of electron donors thus provide conditions favorable to sustain reduction of crystalline Fe(III)-(hydr)oxide reduction.

Alternatively, Fe(III)-(hydr)oxide reduction could proceed through an independent dissolution step, inclusive of ligand promoted dissolution, followed by microbial reduction of $Fe(III)_{aq}$ (26). The reduction of Fe(III) hydrolysis species (and Fe^{3+}) in equilibrium with well-crystalline Fe-(hydr)oxides coupled to the oxidation of hydrogen or acetate may provide sufficient energy for metabolic sustenance, with the caveat that solid-phase dissolution is rapid enough to continuously poise aqueous Fe(III) to activities conducive to continued energy gain. For example, assuming a solution contains a total aqueous Fe(III) activity of 8.0×10^{-12} (aqueous total Fe(III) slightly undersaturated with respect to goethite), 1.0

$\times 10^{-6}$ citrate, and 6.5×10^{-6} Fe^{2+} at pH 7.0, $\text{Fe}(\text{OH})_2^+$ is predicted to be the dominant hydrolysis species in solution, with an activity of 7.20×10^{-12} (calculated using the geochemical modeling program PHREEQC (27)). Under these conditions, reduction of $\text{Fe}(\text{OH})_2^+$ coupled to hydrogen or acetate will yield -136.3 and -322.7 kJ mol^{-1} , respectively. Furthermore, reduction of organically bound Fe(III) will present a viable alternative pathway of Fe(III) reduction (26). Accordingly, Fe(III) citrate_(aq) activity under these conditions is predicted to be 4.2×10^{-15} , and Fe(II)-citrate 8.4×10^{-7} . Even with this high ratio of products to reactants, Fe(III)-citrate is still calculated to be favorable, yielding -7.7 and -355.9 kJ/mol when coupled with hydrogen and acetate oxidation, respectively.

Effect of Mineral Precipitation on Reaction Favorability: Field-Relevant Assessment. While the buildup of metabolites in solution will diminish the thermodynamic favorability of reductive reactions, precipitation of metabolite-bearing solids will exert a strong control on chemical gradients. A number of solid phases may act as Fe(II) sinks and thus affect the Gibbs free energy for a reaction, including magnetite, green rust, siderite, and a number of sulfidic minerals (e.g., mackinawite and pyrite). Siderite is a particularly common Fe(II)-bearing carbonate (FeCO_3) that often imparts controls on Fe^{2+} concentration within soils and sediments, and was identified as a dominant constituent in our sediment profile from Cambodia (SI Figure 3SI). Using a $\log K_{\text{sp}}$ of 0.09 for the reaction:



Fe^{2+} will reach saturation with respect to siderite at an activity of 1.7×10^{-5} under field-relevant conditions (Figure 3). However, Fe^{2+} concentrations are often observed to be higher within soil and sedimentary porewater ($10\text{--}200$ μM) (18), since the concentration necessary for nucleation will be greater than mineral solubility (28). At our field site, Fe^{2+} _(aq) activities range from $\sim 1.0 \times 10^{-6}$ to 2.0×10^{-4} , which fall between ~ 1 and 10 times the values expected for Fe^{2+} saturation with respect to siderite (Figure 3). Thus, it is likely that precipitation of siderite regulates Fe^{2+} _(aq) concentrations within our field site, and prevents (Fe^{2+}) from exceeding 2.0×10^{-4} at the current pH values, which maintains a favorable condition for Fe (hydr)oxide reduction when coupled to acetate (and perhaps hydrogen) oxidation. Variation in bicarbonate activity, however, will alter the solubility of Fe^{2+} with respect to siderite. While average field measurements of bicarbonate activities are $\sim 7.1 \times 10^{-3}$ (and used in our calculations), values range from 2.05×10^{-2} to 4.3×10^{-4} , resulting in Fe^{2+} activities with respect to siderite of 2.1×10^{-5} and 2.9×10^{-4} , which fall within our observed activities of Fe^{2+} (Figure 3).

Sulfate reduction will also impart solubility constraints on metabolite (Fe^{2+} and HS^-) buildup through precipitation of $\text{FeS}_{(\text{s})}$. Precipitation transpires directly through reaction of HS^- with Fe^{2+} ; the solubility of these constituents with respect to $\text{FeS}_{(\text{s})}$ is described by

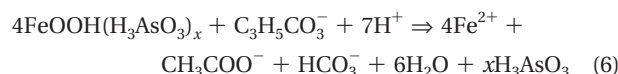


Using a $\log K = -3$ (29), the solubility of HS^- is 1.0×10^{-5} in the presence of 1.0×10^{-5} Fe^{2+} . Low S(-II) is commonly observed in the presence of Fe (hydr)oxides, since S(-II) directly reduces Fe(III)_(s) to Fe(II) and is thus consumed. This also represents an indirect mechanism of iron reduction (source of Fe^{2+}), and may be operative in sediments possessing more recalcitrant Fe(III) (hydr)oxides, such as hematite—minerals less thermodynamically conducive to reduction in the presence of Fe(II). In this reaction sequence, HS^- reduces Fe(III)_(s), producing Fe(II) which may then precipitate as FeS provided additional HS^- is present (30).

These mineralogical constraints on S(-II) and Fe(II), may allow iron and sulfate reduction to occur concurrently, as evidenced by the similar free energies calculated for crystalline Fe (hydr)oxide and sulfate reduction under field conditions (Figure 3). Furthermore, not only does this reaction series remove Fe^{2+} and HS^- , increasing the favorability of both Fe and S reduction, but it also depletes Fe (hydr)oxides, which sorb As, representing another pathway of As mobilization.

Role of Microscale Chemical and Physical Heterogeneity. While the measurements presented herein describe bulk aqueous and soil phase chemical parameters, the heterogeneity of porous media will undoubtedly affect the subsurface distribution of electron donor(s)/acceptor(s), resulting in large microscale variation in biogeochemical thermodynamic favorability. Furthermore, steep chemical gradients develop across cell walls/membranes, likely altering the local (bio)chemical environment and altering free energies accordingly. The influence of such altered environments on thermodynamic favorability remains elusive. Nevertheless, the favorability of overarching biologically driven reactions may be represented by bulk chemical conditions, and certainly are operational for advecting solutes, rendering evaluations of thermodynamic favorability based on such conditions useful for elucidating the predicted ordering of electron acceptor (and donor) utilization. Here, the general sequence of reduction in reduction subsequent to a minimal accumulation of Fe^{2+} is As(V) followed by Fe(III) and S(VI).

Field Site Applicability: Mekong Delta, Cambodia. Iron-(III) (hydr)oxides are strong sorbents of As and thus exert a domineering effect on As mobility (31). The reductive dissolution/transformation of As-bearing Fe(III) (hydr)oxides have been implicated as the likely source of As within many contaminated groundwaters throughout the world, most notably in South and Southeast Asia; the overall reaction liberating As following As(V) reduction to As(III) can be summarized as



where As is bound to Fe-(hydr)oxide (here written as goethite, which is replaceable with other Fe (hydr)oxides), and where x = the stoichiometric coefficient of As (typically very low for South and Southeast Asian sediments, ~ 0.0002). Some As could be incorporated within the lattice structure of the more crystalline (hydr)oxides, such as hematite (32); this fraction of As could remain physically protected from reductive processes until the reductive dissolution of Fe (hydr)oxides. However, within the sediments of our field site, phosphate-extractable As approximates the citrate–bicarbonate–dithionate (CBD) extractable fraction (3), suggesting most of the As is sorbed to mineral surfaces rather than incorporated into the Fe (hydr)oxides.

The binding strength of As on mineral surfaces is partially governed by its speciation, where As(III) is more easily released from Fe(III) (hydr)oxides (33) relative to As(V) (34). Our calculations illustrate that As(V) reduction is more favorable than Fe(III) and S(VI) reduction over a wide-range of field conditions and should thus precede the reduction sequence following marginal Fe(III) reduction to Fe^{2+} , and hence be a key factor in its liberation to the aqueous phase. Within our field sites of the Mekong Delta, goethite, hematite, and within the first 10–50 cm, ferrihydrite, exist as reducible, As-bearing Fe(III) (hydr)oxides (SI Figure 3SI). Throughout the sediment profile, the thermodynamic favorability of As(V) reduction is much greater than Fe(III) (hydr)oxide reduction at measured Fe^{2+} _{aq} concentrations; the only exception being the reduction of ferrihydrite, which yields similar free energy

but is much less prevalent in the flow-field (Figure 3 and SI Figure 3SI). Consistent with this prediction, >80% of the total As is As(III) in all porewater samples collected along the flowpath.

Although As reduction yields the highest energy across a range of field conditions, the reduction of ferrihydrite is also clearly favorable under the conditions measured at our sites (Figure 3). At our field sites, fresh sediments containing ferrihydrite are continuously buried (1–3 mm/yr) during annual inundation, endure repeated cycles of reduction/oxidation above the average seasonal water table (~50–200 cm below ground), and are subjected to anaerobiosis below the seasonal water table—processes conducive to restructuring of Fe(OH)₃ into more crystalline Fe (hydr)oxides. Additionally, Fe(OH)₃ would be utilized preferentially to sulfate and other Fe phases, and would therefore be depleted with time, leading to a dominance of more crystalline phases (e.g., goethite, hematite) which yield less energy when coupled to organic matter oxidation than ferrihydrite (or at Fe²⁺ activities greater than ~5.0 × 10⁻⁵, sulfate reduction) at circumneutral pH (Figures 1–3). In fact, when Fe²⁺ accumulates in soil/sediment porewater, the reduction of hematite becomes biologically *unfavorable* (e.g., it reaches -20 to -10 kJ/mol, the nominal minimum energy required to drive ATP synthesis (35–37); the reaction is microbially unfavorable at Fe²⁺ > 8.0 × 10⁻⁶ when coupled to H₂ oxidation and Fe²⁺ > 3.0 × 10⁻⁴ Fe²⁺ when coupled with acetate oxidation (Figure 1). The unfavorable thermodynamic viability may explain the persistence of hematite below the seasonal water table of our field site (Figure 3, SI Figure 3SI), and may result in longevity of crystalline Fe (hydr)oxides in evolving sediments (38). A more diverse suite of electron donors (e.g., lactate, etc.) would therefore be needed to drive reductive dissolution of As-bearing Fe (hydr)oxides to completion, or Fe(III) must exist in different reducible form (e.g., aqueous hydrolysis species or complexes). Accordingly, As reduction is expected to precede Fe reduction as a mobilization mechanism on a thermodynamic basis. Finally, sulfate reduction may precede Fe(III) reduction in the presence of field-relevant Fe²⁺ concentrations and hematite, as evidenced by diminishing sulfate along a reaction path (SI Figure 3SI)—under these conditions, Fe(III) reduction may then transpire through abiotic (HS⁻) reaction pathways.

Acknowledgments

This work was supported by a U.S. EPA STAR graduate fellowship (EPA-FP916369) and the Stanford NSF Environmental Molecular Sciences Institute (NSF-CHE-0431425). We are grateful to Guangchao Li for laboratory assistance, and are indebted to John Bargar (SSRL) and Sam Webb (SSRL) for their assistance with XAS data collection and analysis. Portions of this research were carried out at the Stanford Synchrotron Radiation Laboratory, a national user facility operated by Stanford University on behalf of the U.S. Department of Energy, Office of Basic Energy Sciences. The SSRL Structural Molecular Biology Program is supported by the Department of Energy, Office of Biological and Environmental Research, and by the National Institutes of Health, National Center for Research Resources, Biomedical Technology Program.

Supporting Information Available

A description of field sampling, mineralogical analysis, and additional Gibbs free energy calculations. This material is available free of charge via the Internet at <http://pubs.acs.org>.

Literature Cited

- (1) Nordstrom, D. K. Public health - Worldwide occurrences of arsenic in ground water. *Science* **2002**, 296 (5576), 2143–2145.

- (2) Smedley, P. L.; Kinniburgh, D. G. A review of the source, behaviour, and distribution of arsenic in natural waters. *Appl. Geochem.* **2002**, 17 (5), 517–568.
- (3) Kocar, B.; Polizzotto, M.; Benner, S.; Ying, S.; Ung, M.; Ouch, K.; Samreth, S.; Suy, B.; Phan, K.; Sampson, M.; Fendorf, S. Integrated biogeochemical and hydrologic processes driving arsenic release from shallow sediments to groundwaters of the Mekong Delta. *Appl. Geochem.* **2008**, 23 (11), 3059–3071.
- (4) Islam, F. S.; Gault, A. G.; Boothman, C.; Poly, D. A.; Charnock, J. M.; Chatterjee, D.; Lloyd, J. R. Role of metal-reducing bacteria in arsenic release from Bengal delta sediments. *Nature* **2004**, 430 (6995), 68–71.
- (5) Nickson, R.; McArthur, J.; Burgess, W.; Ahmed, K. M.; Ravenscroft, P.; Rahman, M. Arsenic poisoning of Bangladesh groundwater. *Nature* **1998**, 395 (6700), 338–338.
- (6) Polizzotto, M.; Kocar, B. D.; Benner, S. B.; Sampson, M.; Fendorf, S. Near-surface wetland sediments as a source of arsenic release to ground water in Asia. *Nature* **2008**, 454 (24 July 2008), 505–508.
- (7) Rosen, B. P. Biochemistry of arsenic detoxification. *Febs Letters* **2002**, 529 (1), 86–92.
- (8) Saltikov, C. W.; Wildman, R. A.; Newman, D. K. Expression dynamics of arsenic respiration and detoxification in *Shewanella* sp strain ANA-3. *J. Bacteriol.* **2005**, 187 (21), 7390–7396.
- (9) Mehta, T.; Coppi, M. V.; Childers, S. E.; Lovley, D. R. Outer membrane c-type cytochromes required for Fe(III) and Mn(IV) oxide reduction in *Geobacter sulfurreducens*. *Appl. Environ. Microbiol.* **2005**, 71 (12), 8634–8641.
- (10) Hartshorne, R. S.; Jepson, B. N.; Clarke, T. A.; Field, S. J.; Fredrickson, J.; Zachara, J.; Shi, L.; Butt, J. N.; Richardson, D. J. Characterization of *Shewanella oneidensis* MtrC: a cell-surface decaheme cytochrome involved in respiratory electron transport to extracellular electron acceptors. *J. Biol. Inorg. Chem.* **2007**, 12 (7), 1083–1094.
- (11) Newman, D. K.; Kolter, R. A role for excreted quinones in extracellular electron transfer. *Nature* **2000**, 405 (6782), 94–97.
- (12) Lovley, D. R.; Blunt-Harris, E. L. Role of humic-bound iron as an electron transfer agent in dissimilatory Fe(III) reduction. *Appl. Environ. Microbiol.* **1999**, 65 (9), 4252–4254.
- (13) Marsili, E.; Baron, D. B.; Shikhare, I. D.; Coursolle, D.; Gralnick, J. A.; Bond, D. R. *Shewanella* secretes flavins that mediate extracellular electron transfer. *Proc. Natl. Acad. Sci. U. S. A.* **2008**, 105 (10), 3968–3973.
- (14) von Canstein, H.; Ogawa, J.; Shimizu, S.; Lloyd, J. R. Secretion of flavins by *Shewanella* species and their role in extracellular electron transfer. *Appl. Environ. Microbiol.* **2008**, 74 (3), 615–623.
- (15) Nevin, K. P.; Lovley, D. R. Mechanisms for Fe(III) oxide reduction in sedimentary environments. *Geomicrobiol. J.* **2002**, 19 (2), 141–159.
- (16) Benner, S. G.; Polizzotto, M.; Kocar, B.; Sampson, M.; Fendorf, S. Groundwater flow in an arsenic-contaminated aquifer, Mekong Delta, Cambodia. *Appl. Geochem.* **2008**, 23 (11), 3072–3087.
- (17) Postma, D.; Jakobsen, R. Redox zonation: Equilibrium constraints on the Fe(III)/SO₄⁻ reduction interface. *Geochim. Cosmochim. Acta* **1996**, 60 (17), 3169–3175.
- (18) Postma, D.; Larsen, F.; Hue, N. T. M.; Duc, M. T.; Viet, P. H.; Nhan, P. Q.; Jessen, S. Arsenic in groundwater of the Red River floodplain, Vietnam: Controlling geochemical processes and reactive transport modeling. *Geochim. Cosmochim. Acta* **2007**, 71, 5054–5071.
- (19) Jakobsen, R.; Postma, D. Redox zoning, rates of sulfate reduction and interactions with Fe-reduction and methanogenesis in a shallow sandy aquifer, Romo, Denmark. *Geochim. Cosmochim. Acta* **1999**, 63 (1), 137–151.
- (20) Hoehler, T. M.; Alperin, M. J.; Albert, D. B.; Martens, C. S. Thermodynamic control on hydrogen concentrations in anoxic sediments. *Geochim. Cosmochim. Acta* **1998**, 62 (10), 1745–1756.
- (21) Jones, D. L. Organic acids in the rhizosphere—A critical review. *Plant Soil* **1998**, 205 (1), 25–44.
- (22) Ratering, S.; Schnell, S. Localization of iron-reducing activity in paddy soil by profile studies. *Biogeochemistry* **2000**, 48 (3), 341–365.
- (23) Stumm, W.; Morgan, J. J., *Aquatic Chemistry: Chemical Equilibria and Rates in Natural Waters*, 3rd ed.; John Wiley and Sons, Inc.: New York, 1996.
- (24) Campbell, K. M.; Malasarn, D.; Saltikov, C. W.; Newman, D. K.; Hering, J. G. Simultaneous microbial reduction of iron(III) and arsenic(V) in suspensions of hydrous ferric oxide. *Environ. Sci. Technol.* **2006**, 40 (19), 5950–5955.

- (25) Lovley, D. R.; Lonergan, D. J. Anaerobic oxidation of toluene, phenol, and para-cresol by the dissimilatory iron-reducing organism, GS-15. *Appl. Environ. Microbiol.* **1990**, *56* (6), 1858–1864.
- (26) Haas, J. R.; Dichristina, T. J. Effects of Fe(III) chemical speciation on dissimilatory Fe(III) reduction by *Shewanella putrefaciens*. *Environ. Sci. Technol.* **2002**, *36* (3), 373–380.
- (27) Parkhurst, D. L.; Appelo, C. A. J. User's Guide to PHREEQC (version 2)—a Computer Program for Speciation, Reaction-Path, 1D-Transport, And Inverse Geochemical Calculations, U.S. Geological Survey Water Resources Investigation Report; U.S. Geological Survey: Reston, VA. **1999**, 99, 99–4259.
- (28) Postma, D. Pyrite and Siderite Formation in Brackish and Fresh-Water Swamp Sediments. *Am. J. Sci.* **1982**, *282* (8), 1151–1183.
- (29) Lindsay, W. L., *Chemical Equilibria in Soils*; John Wiley & Sons: New York, 1979; p 450.
- (30) Poulton, S. W.; Krom, M. D.; Raiswell, R. A revised scheme for the reactivity of iron (oxyhydr)oxide minerals towards dissolved sulfide. *Geochim. Cosmochim. Acta* **2004**, *68* (18), 3703–3715.
- (31) Kinniburgh, D. G.; Smedley, P. L. *Arsenic Contamination of Groundwater in Bangladesh*, WC/00/19; BGS and DPHE, Report WC/00/19; BGS and DPHE: Keyworth, England, 2001.
- (32) Violante, A.; Del Gaudio, S.; Pigna, M.; Ricciardella, M.; Banerjee, D. Coprecipitation of arsenate with metal oxides. 2. Nature, mineralogy, and reactivity of iron(III) precipitates. *Environ. Sci. Technol.* **2007**, *41* (24), 8275–8280.
- (33) Kocar, B. D.; Herbel, M. J.; Tufano, K. J.; Fendorf, S. Contrasting effects of dissimilatory iron(III) and arsenic(V) reduction on arsenic retention and transport. *Environ. Sci. Technol.* **2006**, *40* (21), 6715–6721.
- (34) Manning, B. A.; Goldberg, S. Adsorption and stability of arsenic(III) at the clay mineral-water interface. *Environ. Sci. Technol.* **1997**, *31* (7), 2005–2011.
- (35) Schink, B. Energetics of syntrophic cooperation in methanogenic degradation. *Microbiol. Mol. Biol. Rev.* **1997**, *61* (2), 262–&.
- (36) DeLong, E. F. Life on the thermodynamic edge. *Science* **2007**, *317* (5836), 327–328.
- (37) Jackson, B. E.; McInerney, M. J. Anaerobic microbial metabolism can proceed close to thermodynamic limits. *Nature* **2002**, *415* (6870), 454–456.
- (38) Royer, R. A.; Dempsey, B. A.; Jeon, B. H.; Burgos, W. D. Inhibition of biological reductive dissolution of hematite by ferrous iron. *Environ. Sci. Technol.* **2004**, *38* (1), 187–193.
- (39) Majzlan, J.; Navrotsky, A.; Schwertmann, U., III. Enthalpies of formation and stability of ferrihydrite (similar to Fe(OH)₍₃₎), schwertmannite (similar to Fe(OH)_(3/4)(SO₄)_(1/8)), and epsilon-Fe₂O₃. *Geochim. Cosmochim. Acta* **2004**, *68* (5), 1049–1059.
- (40) Majzlan, J.; Lang, B. E.; Stevens, R.; Navrotsky, A.; Woodfield, B. F.; Boerio-Goates, J. Thermodynamics of Fe oxides: Part I. Entropy at standard temperature and pressure and heat capacity of goethite (alpha-FeOOH), lepidocrocite (gamma-FeOOH), and maghemite (gamma-Fe₂O₃). *Am. Mineral.* **2003**, *88* (5–6), 846–854.
- (41) Cornell, R. M., Schwertmann, U., *The Iron Oxides*, 2nd ed.; Wiley-VCH: Druckhaus Darmstadt, 2003.
- (42) Amend, J. P.; Shock, E. L. Energetics of overall metabolic reactions of thermophilic and hyperthermophilic Archaea and Bacteria. *Fems Microbiol. Rev.* **2001**, *25* (2), 175–243.
- (43) Wagman, D. D.; Evans, W. H.; Parker, V. B.; Schumm, R. H.; Halow, I. *The NBS Tables of Chemical Thermodynamic Properties. Selected Values for Inorganic and C1 and C2 Organic Substances in SI Units*; National Standard Reference Data System: Gaithersburg, MD, 1982.
- (44) Liu, C. G.; Zachara, J. M.; Gorby, Y. A.; Szecsody, J. E.; Brown, C. F. Microbial reduction of Fe(III) and sorption/precipitation of Fe(II) on *Shewanella putrefaciens* strain CN32. *Environ. Sci. Technol.* **2001**, *35* (7), 1385–1393.

ES8035384